

A Novel Generalized Nonlinear Dispersion Equation for Five-Layer Waveguides with Kerr-like Nonlinearity

Jong-Sool Jeong, Seok Ho Song, and El-Hang Lee

CONTENTS

- I. INTRODUCTION
 - II. THEORY
 - III. NUMERICAL RESULTS
 - IV. CONCLUSIONS
- REFERENCES

ABSTRACT

A new method is proposed for the analysis of optical properties of stationary transverse electric (TE) nonlinear waves in the five-layer waveguide which consists of a linear guiding layer with two nonlinear bounding layers sandwiched between a semi-infinite clad and a substrate. By using the relation of the interface electric fields, we obtain the generalized form of nonlinear dispersion equations as an analytic and flexible form. In order to verify the dispersion equation, we apply the dispersion equation to the analysis of the symmetric five-layer waveguide. The nonlinear dispersion curves for several thicknesses of the nonlinear thin film is also presented.

I. INTRODUCTION

Much progress has been made in the studies of nonlinear guided waves exhibiting ultrafast all-optical switching and self-routing characteristics for future telecommunication networks [1], [2]. Special attention has been focused on the three-layer waveguide consisting of a linear thin film bounded by two nonlinear media because it can display several interesting properties, such as self-bending, optical bistability, and generation of spatial solitary waves [3]-[12]. Recently, several different structures have been studied by several authors even though the mathematics are more difficult than that of three-layer waveguide. Sario *et al.* [13], for example, analyzed inhomogeneous four-layer waveguide with a nonlinear medium of finite thickness. Jeong *et al.* [14] analyzed the five-layer nonlinear waveguides having symmetric structures through the dispersion equations obtained by adopting the nonlinear transfer matrix. Lederer *et al.* [15] suggested a tailored multilayer waveguide exhibiting strong nonlinear effects.

In the present work, we propose a new method which can make a complete analysis on the optical properties of stationary transverse electric (TE) nonlinear waves in the five-layer waveguide which consists of a linear guiding layer with two nonlinear bounding layers sandwiched between a semi-infinite clad and a substrate. A generalized, analytic form of a nonlinear dispersion equation is obtained by using the relation of the electric fields at the two interfaces between the upper nonlinear layer and the clad, and between the lower

nonlinear layer and the substrate. To the best of our knowledge, the equation has never been reported before. And an analytical method has not been proposed for the analysis of optical properties in the five-layer nonlinear waveguides having asymmetric structures. The dispersion equation shows a very flexible and general expression because it can be applied to the planar waveguides having a linear core with nonlinear surrounding media and the five-layer nonlinear waveguides having symmetric or asymmetric structures. The five-layer nonlinear waveguide structures have merits that the optical properties, such as optical bistability and power distribution, can be controlled by design of materials and the thicknesses of the linear or the nonlinear thin films. In order to verify the generalized dispersion equation, we apply the equation to the analysis of the typical five-layer waveguide with symmetric structure [14]. Through numerical calculation, it is found that the five-layer waveguide generates three types of modes: (1) asymmetrical, (2) symmetrical, and (3) antisymmetrical. We also present the optical properties as follows: the relation between the mode index and the interface fields, the nonlinear dispersion curves having bifurcation, the power distributions, the behavior of the interface fields for the guided power, and the variation of the nonlinear dispersion curves for several thicknesses of the nonlinear thin film.

II. THEORY

We consider the nonlinear waveguide con-

figuration shown in Fig. 1. It consists of five layers: the linear guiding layer, n_f , of thickness $2a$ between two nonlinear bounding layers covered by semi-infinite clad, n_c , and substrate, n_s , medium. The nonlinear layers of thickness d_{nl1} and d_{nl2} , respectively, have Kerr-like refractive indices of $n_i^2 = \bar{n}_i^2 + \alpha_i |E_i|^2$ ($i = 1, 2$) where E_i is an amplitude of the electric field in medium i , \bar{n}_i , the linear refractive index, and α_i , the nonlinear coefficient of the Kerr-like film. For simplicity, we consider the self-focusing nonlinear medium ($\alpha_i > 0$) and neglect the absorption effect of the medium.

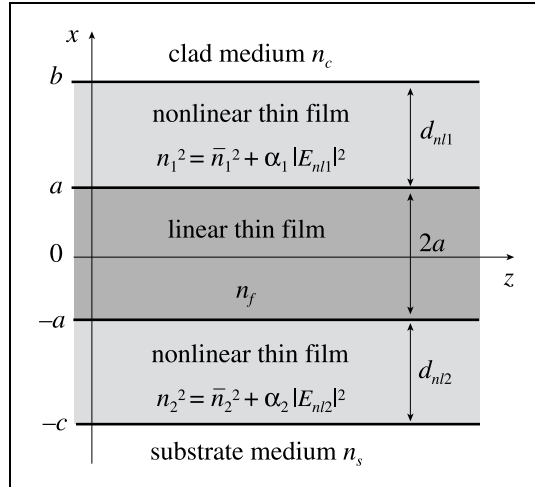


Fig. 1. Schematic drawing of the nonlinear waveguide bounded by two nonlinear layers sandwiched by a semi-infinite clad and a substrate.

Our analysis is restricted to TE waves propagating along the z direction. The TE field may be written as

$$F_i(x, z, t) = \frac{1}{2} E_i(x) \exp[j(\omega t - k_0 \beta z)] + \text{c.c.} \quad (1)$$

with the mode index of β and the free-space

wave number of k_0 . The governing equation for the electric field E_i in the i th nonlinear medium is given by

$$\frac{d^2}{dx^2} E_i(x) + k_0^2 [(\bar{n}_i^2 - \beta^2) + \alpha_i |E_i(x)|^2] E_i(x) = 0. \quad (2)$$

The first integration of (2) gives

$$\frac{1}{k_0^2} \left(\frac{dE_i(x)}{dx} \right)^2 + \left[(\bar{n}_i^2 - \beta^2) + \frac{\alpha_i}{2} E_i^2(x) \right] E_i^2(x) = C_{nli}. \quad (3)$$

At the interfaces $x = b$ and $x = -c$, respectively, the integration constant C_{nli} is given as follows [16]:

$$C_{nli} = (\bar{n}_i^2 - n_{c,s}^2) E_{0i}^2 + \frac{1}{2} \alpha_i E_{0i}^4 \quad (4)$$

with the clad (substrate) refractive index n_c (n_s) and the electric field E_{0i} at the interfaces $x = b$ and $x = -c$, respectively. The electric field $E_{nli}(x)$ of the i th nonlinear thin film can be expressed by Jacobian elliptic function [16]-[18]

$$E_{nli}(x) = p_i \text{cn}[k_0 q_i (x + x_{0i}) | m_i], \quad (5)$$

where x_{0i} is an integration constant indicating the location of the maximum field, $p_i = q_i \sqrt{2m_i/\alpha_i}$, $q_i^2 = (\bar{n}_i^2 - \beta^2)(1/2m_i)$, $m_i = (|\Gamma_i| - (\bar{n}_i^2 - \beta^2))/2|\Gamma_i|$, and $\Gamma_i^2 = (\bar{n}_i^2 - \beta^2)^2 + 2\alpha_i C_{nli}$. From the relation of the tangential components of the field and its derivative at the interfaces $x = b$ and $x = -c$, respectively, we find the relation obtaining the integration constant x_{0i} as follows:

$$\text{sn}^2(k_0 q_i x_{0i} | m_i) = \frac{(1 + \zeta_i) - [(1 + \zeta_i)^2 - 4m_i \zeta_i]^{1/2}}{2m_i} \quad (6)$$

with $\zeta_i = (2m_i - 1)(\beta^2 - n_{c,s}^2)(\beta^2 - \bar{n}_i^2)^{-1}$.

The electric fields in the waveguide, consisting of five layers, are

$$\begin{aligned} E_c(x) &= E_{01} \exp(-k_0 \gamma_c (x-b)) & x > b \\ E_{nl1}(x) &= p_1 \operatorname{cn}[k_0 q_1 (x-b+x_{01}) | m_1] \\ & & b > x > a \end{aligned}$$

$$\begin{aligned} E_f(x) &= \\ & \begin{cases} A \cos(k_0 \gamma_f (x-a)) + B \sin(k_0 \gamma_f (x-a)) \\ \quad \text{for } n_f > \beta \\ A \cosh(k_0 \gamma_f (x-a)) + B \sinh(k_0 \gamma_f (x-a)) \\ \quad \text{for } n_f < \beta \end{cases} \\ & & a > x > -a \end{aligned}$$

$$\begin{aligned} E_{nl2}(x) &= p_2 \operatorname{cn}[k_0 q_2 (x+c-x_{02}) | m_2] \\ & & -a > x > -c \end{aligned}$$

$$E_s(x) = E_{02} \exp(k_0 \gamma_s (x+c)) \quad -c > x \quad (7)$$

with $\gamma_f = \sqrt{|n_f^2 - \beta^2|}$, $\gamma_c = \sqrt{\beta^2 - n_c^2}$, $\gamma_s = \sqrt{\beta - n_s^2}$.

After appropriately manipulating the conservation constants, we can obtain the relation between the interface electric fields E_{01} and E_{02} in the five-layer waveguides with either symmetric or asymmetric structure. At the interface $x=a$, the boundary conditions provide

$$\begin{aligned} A &= p_1 \operatorname{cn}[k_0 q_1 (a-b+x_{01}) | m_1] \\ \gamma_f B &= -p_1 q_1 \operatorname{sn}[k_0 q_1 (a-b+x_{01}) | m_1] \\ & \quad \times \operatorname{dn}[k_0 q_1 (a-b+x_{01}) | m_1]. \quad (8) \end{aligned}$$

At the interface $x=-a$, the field and its deriva-

tive are given by

$$\begin{aligned} E_{nl2}(x) \Big|_{x=-a} &= \\ & \begin{cases} A \cos(2ak_0 \gamma_f) - B \sin(2ak_0 \gamma_f) & \text{for } n_f > \beta, \\ A \cosh(2ak_0 \gamma_f) - B \sinh(2ak_0 \gamma_f) & \text{for } n_f < \beta, \end{cases} \quad (9) \end{aligned}$$

$$\begin{aligned} \frac{d}{dx} E_{nl2}(x) \Big|_{x=-a} &= \\ & \begin{cases} k_0 \gamma_f [A \sin(2ak_0 \gamma_f) + B \cos(2ak_0 \gamma_f)] \\ \quad \text{for } n_f > \beta, \\ k_0 \gamma_f [-A \sinh(2ak_0 \gamma_f) + B \cosh(2ak_0 \gamma_f)] \\ \quad \text{for } n_f < \beta, \end{cases} \quad (10) \end{aligned}$$

with (8). By substituting (9) and (10) into (3), we obtain the conservation constant $C_{nl2} \Big|_{x=-a}$ at the interface $x=-a$ as follows:

$$\begin{aligned} C_{nl2} \Big|_{x=-a} &= \\ & \begin{cases} |n_f^2 - \beta^2| (A \sin \theta + B \cos \theta)^2 \\ \quad + (\bar{n}_2^2 - \beta^2) (A \cos \theta - B \sin \theta)^2 \\ \quad + \frac{1}{2} \alpha_2 (A \cos \theta - B \sin \theta)^4 \\ \quad \text{for } n_f > \beta, \\ |n_f^2 - \beta^2| (A \sinh \theta - B \cosh \theta)^2 \\ \quad + (\bar{n}_2^2 - \beta^2) (A \cosh \theta - B \sinh \theta)^2 \\ \quad + \frac{1}{2} \alpha_2 (A \cosh \theta - B \sinh \theta)^4 \\ \quad \text{for } n_f < \beta, \end{cases} \quad (11) \end{aligned}$$

with $\theta = 2ak_0 \gamma_f$. And the conservation constant $C_{nl2} \Big|_{x=-c}$ at the interface $x=-c$ is given

by

$$C_{nl2}|_{x=-c} = (\bar{n}_2^2 - n_s^2)E_{02}^2 + \frac{1}{2}\alpha_2 E_{02}^4, \quad (12)$$

as shown in (4). Since the conservation constant describing the relation between the electric field and its derivative has the same value at any point of the nonlinear thin film as shown in (3), we can take the equation

$$C_{nl2} = C_{nl2}|_{x=-a} = C_{nl2}|_{x=-c}. \quad (13)$$

With the help of (11)-(13), we can obtain the relation of the E_{02} and $C_{nl2}|_{x=-a}$ as follows:

$$\alpha_2 E_{02}^2 = -(\bar{n}_2^2 - n_s^2) + ((\bar{n}_2^2 - n_s^2)^2 + 2\alpha_2 C_{nl2}|_{x=-a})^{1/2}. \quad (14)$$

(14) is utilized to calculate the interface fields E_{01} and E_{02} corresponding to the mode condition in the five-layer waveguide including asymmetric two nonlinear bounding layers.

Applying the boundary conditions for the fields and its derivatives at each interface, we find the dispersion equations determining the power-dependent mode. At the boundary $x = -a$,

for $n_f > \beta$,

$$\begin{aligned} A \cos \theta - B \sin \theta &= p_2 \text{cn}[k_0 q_2 (c - a - x_{02}) | m_2] \\ \gamma_f (A \sin \theta + B \cos \theta) &= -p_2 q_2 \text{sn}[k_0 q_2 (c - a - x_{02}) | m_2] \\ &\quad \times \text{dn}[k_0 q_2 (c - a - x_{02}) | m_2] \end{aligned} \quad (15)$$

for $n_f < \beta$,

$$\begin{aligned} A \cosh \theta - B \sinh \theta &= p_2 \text{cn}[k_0 q_2 (c - a - x_{02}) | m_2] \\ \gamma_f (-A \sinh \theta + B \cosh \theta) &= -p_2 q_2 \text{sn}[k_0 q_2 (c - a - x_{02}) | m_2] \\ &\quad \times \text{dn}[k_0 q_2 (c - a - x_{02}) | m_2]. \end{aligned} \quad (16)$$

Setting $u_1 = k_0 q_1 (a - b + x_{01})$ and $u_2 = k_0 q_2 (c - a - x_{02})$, and with the help of (8), (15), and (16), a generalized form of the dispersion equation is given by

$$\tan \theta = \frac{U_1(\beta, E_{01}) - U_2(\beta, E_{02})}{(-1)^h + U_1(\beta, E_{01})U_2(\beta, E_{02})}, \quad (17)$$

where

$$U_i(\beta, E_{0i}) = \frac{q_i \text{sn}(u_i | m_i) \text{dn}(u_i | m_i)}{\gamma_f \text{cn}(u_i | m_i)} \quad (18)$$

with the parameter h indicating the integer 0 or 1. (17) is valid with $h = 0$ for $n_f > \beta$. In the case of $n_f < \beta$, it can be readily shown that (17) is valid with \tan replaced by \tanh and $h = 1$. The dispersion equation of (17) has been obtained by using (14) describing the relation between the electric fields of E_{01} and E_{02} at the two interfaces between the upper nonlinear layer and the clad, and between the lower nonlinear layer and the substrate. And the term of $\text{sn}(u|m)\text{dn}(u|m)/\text{cn}(u|m)$ in (18) is a very flexible and general expression because it can describe the linear layer, the nonlinear layer, the linear media, and the nonlinear media. The dispersion equation of (17), therefore, shows a generalized form, which can be applied to the planar waveguides having a linear core with nonlinear surrounding media and the five-layer nonlinear waveguides having symmetric or asymmetric structures. In the case of $\alpha_i = 0$ and $\bar{n}_i = n_{c,s}$, $U_i(\beta, E_{0i})$ becomes q_i/γ_f due to $m_i = 1$ and $x_{0i} \rightarrow \infty$, which is obtained from (6), and therefore (17) becomes the dispersion equation for the three-layer linear waveguide. And in the case of $b, c \rightarrow \infty$, $U_i(\beta, E_{0i})$

approaches $q_i \tanh(u_i)/\gamma_i$ with $m_i \rightarrow 1$, $(b - x_{01}) \rightarrow x'_{01}$, and $(c - x_{02}) \rightarrow x'_{02}$, and (17) is simplified to the dispersion equation of the three-layer nonlinear waveguide presented by Seaton *et al.* [3]. In this approach the power-dependent mode index β and the interface electric fields become the vital parameters of the nonlinear dispersion equation. After fixing the mode index β , we can find the interface electric fields with (14) and (17) by using the shooting and matching technique. The pairs of β and the interface electric fields are then utilized to plot the nonlinear dispersion curve which depicts the dependence of the mode indices on the total guided power.

The total guided power P_{total} per unit width is given by the power-dependent mode index β and the interface fields as follows:

$$\begin{aligned} P_{total} &= \frac{1}{2} \eta_0 \beta \int_{-\infty}^{\infty} E^2(x) dx \\ &= P_{nl1} + P_{lin} + P_{nl2} \\ &\quad + \frac{\beta \eta_0}{4k_0} \left(\frac{E_{01}^2}{\sqrt{\beta^2 - n_c^2}} + \frac{E_{02}^2}{\sqrt{\beta^2 - n_s^2}} \right) \end{aligned} \quad (19)$$

where η_0 is the free space admittance, P_{lin} is the fraction of the power propagating within the linear guiding layer, and P_{nl1} and P_{nl2} are those within the upper and lower nonlinear bounding layers, respectively. The guided power P_{lin} in the linear guiding layer can be obtained in the analytical forms as follows:

$$\begin{aligned} P_{lin} &= \frac{\eta_0 \beta}{8k_0 \gamma_f} [4Q_0 k_0 \gamma_f a + Q_1 \sin(2\theta) + Q_2 \sin^2 \theta] \\ &\quad \text{for } n_f > \beta, \end{aligned}$$

$$\begin{aligned} P_{lin} &= \frac{\eta_0 \beta}{8k_0 \gamma_f} [4Q_1 k_0 \gamma_f a + Q_0 \sinh(2\theta) + Q_2 \sinh^2 \theta] \\ &\quad \text{for } n_f < \beta, \end{aligned} \quad (20)$$

with $Q_0 = AA^* + BB^*$, $Q_1 = AA^* - BB^*$, $Q_2 = -2(AB^* + BA^*)$ where the constants A and B are given by (8). In the upper and lower nonlinear bounding layers, the nonlinear powers $P_{nli(i=1,2)}$ are also obtained by

$$P_{nli} = \frac{1}{2} \eta_0 \beta p_i^2 \int_0^{d_{nli}} \text{cn}^2[k_0 q_i(x + x_{0i}) | m_i] dx. \quad (21)$$

III. NUMERICAL RESULTS

We will investigate the verification of the generalized dispersion equation by analyzing the typical five-layer waveguide structure [14] having two symmetric self-focusing nonlinear layers. The employed parameters are as follows: $\bar{n}_1 = \bar{n}_2 = 1.55$, $n_c = n_s = 1.50$, $n_f = 1.570$, $\alpha_1 = \alpha_2 = 6.38 \times 10^{-12} \text{m}^2/\text{V}^2$ (MBBA liquid crystal), $\lambda = 0.515 \mu\text{m}$, $a = 0.6 \mu\text{m}$, and $d_{nl1} = d_{nl2} = 1.0 \mu\text{m}$. The optical properties are presented as follows: the relation between the mode index and the interface fields, the nonlinear dispersion curves having bifurcation, the power distributions, and the behavior of the interface fields for the guided power.

Figure 2 shows the relations between two interface field intensities, E_{01}^2 and E_{02}^2 , where we used three different values of the mode index β as a parameter: the solid curve for $\beta = 1.567$, the dashed curve for $\beta = 1.568$, and the dashed-and-dotted curve for $\beta = 1.569$, re-

spectively. The curves are similar to those of polynomial equation of the fourth degree. As shown in Fig. 2, the curves have three regions in the real part of the electric fields, i.e., $E_{02}^2 > 0$. We, therefore, can predict that the five-layer waveguides generate three types of modes.

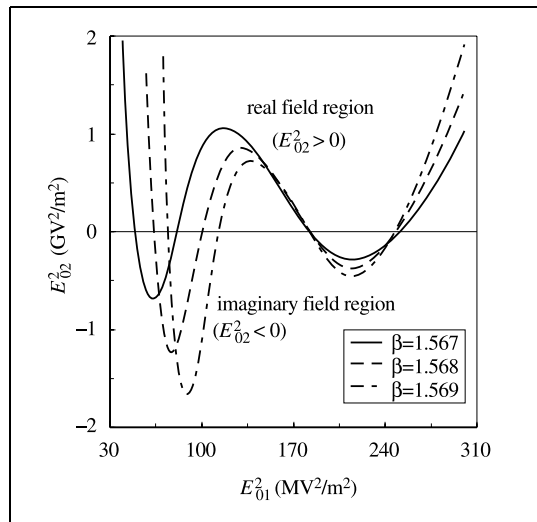


Fig. 2. Relations between two interface field intensities, E_{01}^2 and E_{02}^2 , where the mode index β is used as a parameter: the solid curve for $\beta = 1.567$, the dashed curve for $\beta = 1.568$, and the dashed-and-dotted curve for $\beta = 1.569$, respectively.

Figure 3 illustrates the interface field intensity corresponding to the mode condition in the interface fields shown in Fig. 2. The figure shows the dependence of the interface field intensity E_{02}^2 on the mode index for three types of modes: the asymmetrical (the solid curve), the symmetrical (the dashed curve), and the antisymmetrical (the dashed-and-dotted curve), respectively. The dashed vertical line indicates the mode index corresponding to the re-

fractive index of the linear guiding layer. For $\beta = 1.5656$, the asymmetrical modes and the symmetrical modes are bifurcated each other. The turnaround point of E_{02}^2 occurs at a value higher than n_f for the asymmetrical modes and the symmetrical modes, but it occurs at lower value for the antisymmetrical modes.

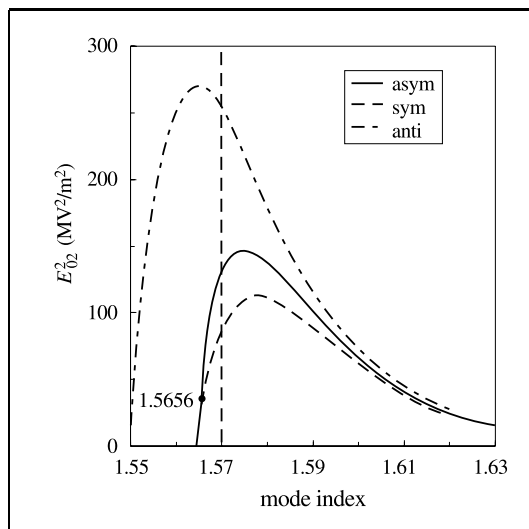


Fig. 3. Dependence of the interface field intensity E_{02}^2 on the mode index for three types of modes: the asymmetrical (the solid curve), the symmetrical (the dashed curve), and the antisymmetrical (the dashed-and-dotted curve), respectively.

Figure 4 shows the nonlinear dispersion curves for three types of solutions: the solid curve for the asymmetrical modes, the dashed curve for the symmetrical modes, and the dashed-and-dotted curve for the antisymmetrical modes, respectively. It is interesting to note that the asymmetric branch bifurcates from the symmetric one, as was in case of the three-layer nonlinear waveguide [3]. And

the dispersion curve of the antisymmetrical modes shows that the mode indices increase almost linearly with the guided power. It has been shown theoretically that the symmetrical mode and the asymmetrical nonlinear mode on the negatively sloped branch of the dispersion curve is unstable in the three-layer nonlinear waveguides [9]. But the stability of three types of modes generated in the five-layer waveguides should be checked using the propagating beam method or the mathematical stability technique [9], [10].

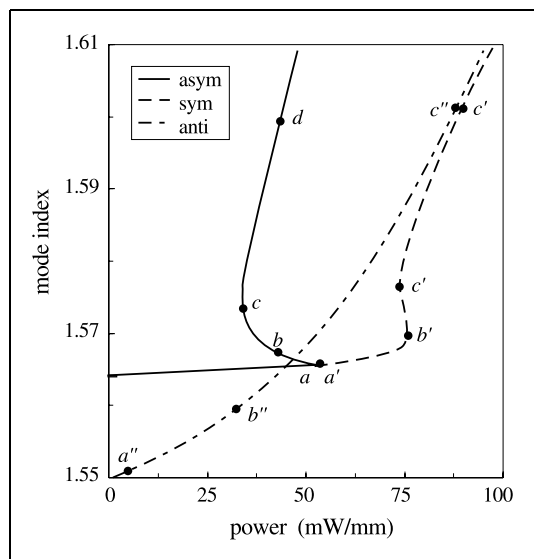


Fig. 4. Nonlinear dispersion curves for three types of solutions: the solid curve for the asymmetrical modes, the dashed curve for the symmetrical modes, and the dashed-and-dotted curve for the antisymmetrical modes, respectively.

Figure 5 shows the field distributions at some points on the dispersion curves of Fig. 4. For the asymmetrical mode shown in Fig. 5(a), until the guided power reaches the threshold

value of $P_{th} \approx 52.96$ mW/mm, the field is essentially confined within the linear guiding layer and it gradually moves to either one of two nonlinear layers as the mode index increases. Figure 5(b) shows for the symmetrical modes that until the power reaches $P_{th} \approx 75.88$ mW/mm, the field remains flat in the linear layer and then the field maximum suddenly splits into two peaks, both of which exist within the nonlinear layers. The antisymmetrical modes plotted in Fig. 5(c), however, the field maximum of the mode cannot exist within the linear layer even at the mode index lower than the refractive index of the linear layer.

Figure 6 illustrates the variation of the integration constant x_{02} as a function of the mode index for three types of modes: the asymmetrical (the solid curve), the symmetrical (the dashed curve), and the antisymmetrical (the dashed-and-dotted curve), respectively. For $x_{02} < 1.0$ μm the field maximum locates within the nonlinear bounding layer, but for $x_{02} > 1.0$ μm the field maximum exists within the linear guiding layer. It is interesting to note that for the asymmetrical modes and the antisymmetrical modes, the field maximum locates within the nonlinear region even in case of $\beta < n_f$.

Figure 7 depicts the optical bistable properties of the power distributions between the fraction of the power in the linear guiding layer, P_{lin} , and that of the power in the nonlinear bounding layers, P_{nl} , with respect to the total guided power, P_{total} , for three types of modes. Most of the power propagates in the linear film up to the threshold power of $P_{th} \approx 52.96$ mW/mm for asymmetrical modes

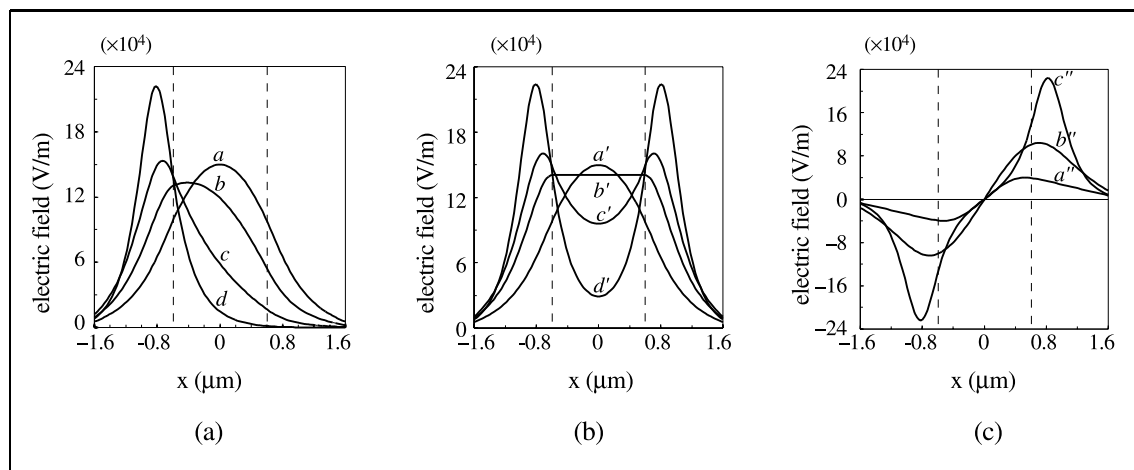


Fig. 5. Field distributions at some points on the dispersion curves of Fig. 4: (a) the asymmetrical modes, (b) the symmetrical modes, and (c) the antisymmetrical modes, respectively.

and up to $P_{th} \approx 75.88$ mW/mm for symmet-

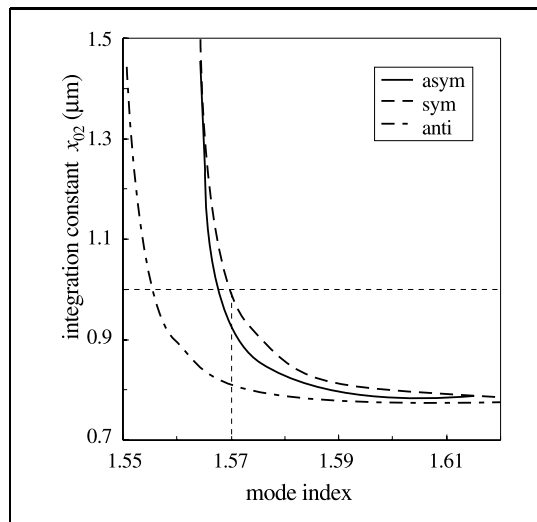


Fig. 6. Variation of the integration constant x_{02} as a function of the mode index for three types of modes: the asymmetrical (the solid curve), the symmetrical (the dashed curve), and the antisymmetrical (the dashed-and-dotted curve), respectively.

rical modes. With further increase beyond the threshold power, the propagating power is transferred from the linear guiding layer into the nonlinear bounding layers because the refractive indices of the nonlinear layers increase with the power. It should be noted that these bistable curves are similar to the bistable characteristics of a nonlinear Fabry-Perot etalon. Figure 8 shows the relations between the interface field intensity and the guided power, and it is shown that the interface field intensity of the asymmetrical modes and the symmetrical modes has the bistable behaviors for the guided power.

Now, we consider the optical nonlinear properties for the variation of the nonlinear film thickness with the fixed thickness of the linear film. Figure 9 shows the variation of the nonlinear dispersion curves for several thicknesses of the nonlinear thin film with $a = 0.5 \mu\text{m}$ and $d_{nl2} = 0 \mu\text{m}$. The solid curve gives

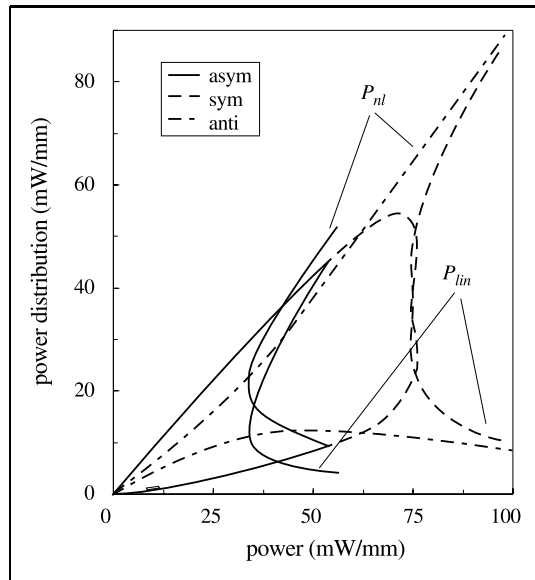


Fig. 7. Power distributions between the fraction of the power in the linear guiding layer, P_{lin} , and that of the power in the nonlinear bounding layers, P_{nl} , for three types of modes.

the optical bistability of the mode indices for the nonlinear film thickness of $d_{nl1} = 1.0 \mu\text{m}$, the dashed curve for $d_{nl1} = 0.4 \mu\text{m}$, and the dashed-and-dotted curve for $d_{nl1} = 0.3 \mu\text{m}$, respectively. It has been found that the optical bistabilities are exhibited and the critical powers for the optical bistability are increased with the decrease of the thickness of the nonlinear thin film, as shown in Fig. 9.

IV. CONCLUSIONS

In conclusion, we have proposed a novel, generalized method to analyze the optical properties of the nonlinear guided waves

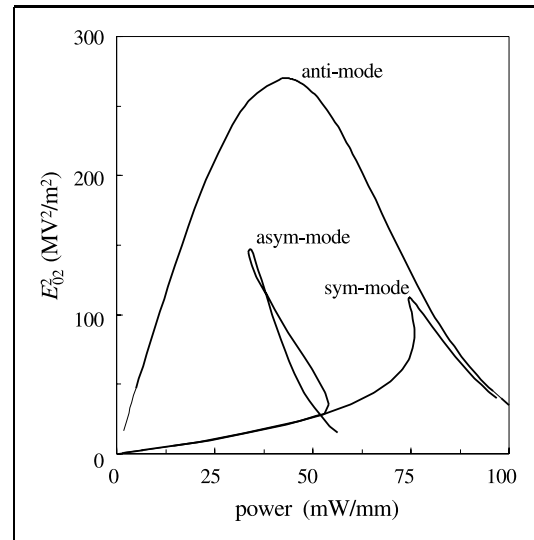


Fig. 8. Optical relations between the interface field intensity and the guided power for three types of modes.

in the nonlinear waveguides, which consist of five layers. The new form of nonlinear dispersion equation, which is based on the relation between the interface fields, has been obtained in analytic form. The dispersion equation shows a very flexible and general expression because it can be applied to the planar waveguides having a linear core with nonlinear surrounding media and the five-layer nonlinear waveguides having symmetric or asymmetric structures. In order to verify the dispersion equation, we have analyzed the optical properties of the typical five-layer waveguide with symmetric structure. We have learned that the five-layer waveguide generates three types of modes: the asymmetrical, the symmetrical, and the antisymmetrical modes. It has been found that the nonlinear

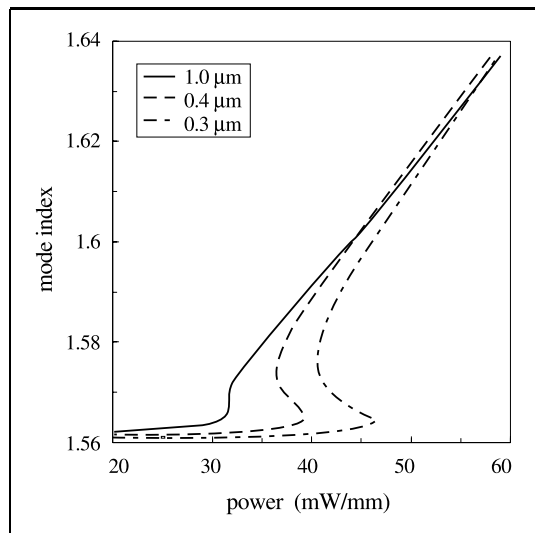


Fig. 9. Variation of nonlinear dispersion curves for several thicknesses of the nonlinear thin film: the solid curve gives the nonlinear mode indices for the nonlinear film thickness of $d_{nl1} = 1.0 \mu\text{m}$, the dashed curve, $d_{nl1} = 0.4 \mu\text{m}$, and the dashed-and-dotted curve, $d_{nl1} = 0.3 \mu\text{m}$, respectively.

dispersion curve is bifurcated into the asymmetric branch and the symmetric branch, as was in case of the three-layer nonlinear waveguide. The dependence of the field maximum location upon the mode index was also presented. And the power distributions and the interface electric fields display optical bistable behaviors, which are similar to those of a nonlinear Fabry-Perot etalon. We have also found that the optical bistabilities are exhibited and the critical powers for the optical bistability are increased with the decrease of the thickness of the nonlinear thin film.

We employed the parameters of MBBA liquid crystal as a nonlinear medium. How-

ever, the liquid crystal exhibits a large loss and very slow nonlinearity, due to its thermal nature. Hence, it is not suitable for all-optical applications. Therefore, we consider another several nonlinear media, such as single crystal P-toluene sulphonate (PTS), heterocyclic ladder polymer, ion-exchanged $\text{CdS}_{1-x}\text{Se}_x$ -doped glass, Sn-doped silica glass by ion implantation, and Gold ion implanted glass.

REFERENCES

- [1] G. I. Stegeman, E. M. Wright, N. Finlayson, R. Zanoni, and C. T. Seaton, "Third order nonlinear integrated optics," *J. Lightwave Tech.*, vol. LT-6, pp. 953-970, 1988.
- [2] A. B. Aceves, P. Varatharajah, A. C. Newell, E. M. Wright, G. I. Stegeman, D. R. Heatley, J. V. Moloney, and H. Adachihara, "Particle aspects of collimated light channel propagation at nonlinear interfaces and in waveguides," *J. Opt. Soc. Am. B*, vol. 7, pp. 963-974, 1990.
- [3] C. T. Seaton, J. D. Valera, R. L. Shoemaker, G. I. Stegeman, J. T. Chilwell, and S. D. Smith, "Calculations of nonlinear TE waves guided by thin dielectric films bounded by nonlinear media," *IEEE J. Quantum Electron.*, vol. QE-21, pp. 774-783, 1985.
- [4] A. D. Boardman and P. Egan, "S-Polarized waves in a thin dielectric film asymmetrically bounded by optically nonlinear media," *IEEE J. Quantum Electron.*, vol. QE-21, pp. 1701-1713, 1985.
- [5] A. Ankiewicz and H. T. Tran, "A new class of nonlinear guided waves," *J. Mod. Opt.*, vol. 38, pp. 1093-1106, 1991.
- [6] J. P. Torres and L. Torner, "Universal diagrams for TE waves guided by thin films bounded by saturable nonlinear media," *IEEE J. Quantum Electron.*, vol. QE-29, pp. 917-925, 1993.

- [7] K. S. Chiang and R. A. Sammut, "Iterative methods and stability of TE modes of nonlinear planar waveguides," *Opt. Commun.*, vol. 109, pp. 59-64, 1994.
- [8] J. P. Torres and L. Torner, "Diagrammatic analysis of nonlinear planar waveguides," *J. Opt. Soc. Am. B*, vol. 11, pp. 45-52, 1994.
- [9] C. K. R. T. Jones and J. V. Moloney, "Instability of standing waves in nonlinear optical waveguides," *Phys. Lett. A*, vol. 117, pp. 175-180, 1986.
- [10] J. Atai and Y. Chen, "Stability of the asymmetric nonlinear mode trapped in symmetric planar waveguides," *J. Lightwave Tech.*, vol. LT-11, pp. 577-581, 1993.
- [11] L. Leine, C. Wchter, U. Langbein, and F. Lederer, "Evolution of nonlinear guided optical fields down a dielectric film with a nonlinear cladding," *J. Opt. Soc. Am. B*, vol. 5, pp. 547-558, 1988.
- [12] C. De Angelis and G. F. Nalesso, "Spatial soliton switching modes of nonlinear optical slab waveguides," *J. Opt. Soc. Am. B*, vol. 10, pp. 55-59, 1993.
- [13] M. De Sario, A. D'Orazio, V. Petruzzelli, and F. Prudenzano, "Propagation characteristics of nonlinear graded-index optical waveguides," *J. Opt. Soc. Am. B*, vol. 10, pp. 1565-1571, 1993.
- [14] J.-S. Jeong, C. H. Kwak, and E.-H. Lee, "Optical properties of TE nonlinear waves in planar waveguides with two nonlinear bounding layers," *Opt. Commun.*, vol. 116, pp. 351-357, 1995.
- [15] F. Lederer, L. Leine, R. Muschall, T. Peschel, C. Schmidt-Hattenberger, U. Trutschel, A. D. Boardman, and C. Wchter, "Strongly nonlinear effects with weak nonlinearities in smart waveguides," *Opt. Commun.*, vol. 99, pp. 95-100, 1993.
- [16] A. D. Boardman and P. Egan, "Optically nonlinear waves in thin films," *IEEE J. Quantum Electron.*, vol. QE-22, pp. 319-324, 1986.
- [17] N. N. Akhmediev, K. O. Bolter, and V. M. Eleonskii, "Optical dielectric waveguide with nonlinear permittivity," *Opt. Spectrosc.*, vol. 53, pp. 540-542, 1982.
- [18] Y.-F. Li and K. Iizuka, "Unified nonlinear waveguide dispersion equations without spurious roots," *IEEE J. Quantum Electron.*, vol. QE-31, pp. 791-794, 1995.

Jong-Sool Jeong was born in Chinju, Korea on August 28, 1967. He received the B.E. and M.E. degrees in electronics engineering from Pusan National University, Korea, in 1990 and 1992, respectively. Since 1992

he has been involved in the basic research at Electronics and Telecommunications Research Institute (ETRI) in Taejon, Korea. His current research interests include all-optical operation, optical communication, nonlinear optical phenomena, and finite-difference time-domain (FDTD) modeling.

Seok Ho Song received his B.S. degree in the Department of Physics from Yonsei University in 1984. He obtained his M.S. degree in 1986 and Ph.D. in 1989 both from the Department of Physics, Korean Advanced Institute of Science and Technology (KAIST), Seoul, Korea. Since 1989 he has been involved in the basic research at Electronics and Telecommunications Research Institute (ETRI) in Taejon. He spent one year (1991) at the University College London as a visiting scientist. He has been working on optical interconnections, diffractive optics, and optical parallel switching and computing. His recent research interests include micro-optics and 3-dimensionally integrated planer optics. He is a member of the Optical Society of America, the IEEE/LEOS, the Korean Optical Society, and the Korean Physics Society.

El-Hang Lee
See *ETRI Journal*, vol. 17, no. 2, p. 10, July 1995.